An Insertion Mutation Located on Putative Enhancer Regions of the *MYB26*-Like Gene Induce Inhibition of Anther Dehiscence Resulting in Novel Genic Male Sterility in Radish (*Raphanus Sativus* L.)

Seongjun Kim
Chonnam National University College of Agriculture and Life Sciences
Sunggil Kim (dronion@jnu.ac.kr)
Chonnam National University https://orcid.org/0000-0001-8555-2995

Research Article

Keywords: Radish (Raphanus sativus L.), Genic male-sterility, Anther dehiscence, MYB26 transcription factor, Functional marker

Posted Date: July 7th, 2021

DOI: https://doi.org/10.21203/rs.3.rs-626059/v1

Abstract

A novel male-sterility trait was identified in a radish (*Raphanus sativus* L.) population. Although the size of male-sterile anthers was comparable to that of normal flowers, no pollen grain was observed during anther dehiscence. However, dissection of male-sterile anthers revealed an abundance of normal pollen grains. Analysis of segregating populations showed that a single recessive locus, designated *RsMs1* conferred male sterility. Based on two radish draft genome sequences, molecular markers were developed to delimit the genomic region harboring the *RsMs1*. The region was narrowed down to approximately 27 kb after analyzing recombinants selected from 7,511 individuals of a segregating population. Sequencing of the delimited region yielded six putative genes including four genes expressed in the floral tissue, and one gene with significant differential expression between male-fertile and male-sterile individuals of a segregating population. This differentially expressed gene was orthologous to the *Arabidopsis MYB26* gene, which played a critical role in anther dehiscence. Excluding a synonymous single nucleotide polymorphism in exon3, no polymorphism involving coding and putative promoter regions was detected between alleles. A 955-bp insertion was identified 7.5 kb upstream of the recessive allele. Highly conserved motifs among four Brassicaceae species were identified around this insertion site, suggesting the presence of putative enhancer sequences. A functional marker was developed for genotyping of the *RsMs1* based on the 955-bp insertion. A total of 120 PI accessions were analyzed using this marker, and 11 accessions were shown to carry the recessive *RsMs1* allele.

Introduction

Sexual reproduction in plants is facilitated by the anther primordium derived from floral meristem, and the maturation of anther occurs via 14 developmental stages in both eudicot *Arabidopsis* (Sanders et al. 1999) and monocot rice (Zhang et al. 2011). Wan et al. (2019) classified these 14 stages into four major phases: archesporial cell specification (stages 1–2), anther somatic cell division (stages 3–5), tapetum development and pollen mother cell meiosis (stages 6–8), and mature pollen formation and anther dehiscence (stages 9–14). Defects in all 14 developmental stages occasionally result in male sterility in which functional pollen grains are not formed or released during anther dehiscence (Wan et al. 2019).

Male sterility is classified into cytoplasmic male sterility (CMS) and genic male sterility (GMS) depending on genomic locations of the causal genes. CMS is caused by aberrant genes in the mitochondrial genomes. These genes are mostly chimeric genes created by dynamic rearrangement of plant mitochondrial genomes (Schnable and Wise 1998; Budar et al. 2003; Hanson and Bentolila 2004; Kim and Zhang 2018). Naturally occurring CMS is widely distributed in plants, which may increase genetic diversity of populations (Laser and Lersten 1972). Male fertility of CMS can be frequently restored by nuclear genes known as restorer-of-fertility (Rf) genes. The majority of Rf genes are known to encode pentatricopeptide repeat (PPR) proteins (Bentolila et al. 2002; Brown et al. 2003; Komori et al. 2004; Klein et al. 2005; Gaborieau et al. 2016).

Meanwhile, GMS is caused by nuclear genes involved in anther development. At least 40 genes causing GMS have been reported in *Arabidopsis* and rice, respectively. Among them, 17 genes are known to be orthologous between *Arabidopsis* and rice (Wan et al. 2019). The anther wall consists of four cell layers: epidermis, endothecium, middle layer, and tapetum. The tapetum surrounding the developing microspores plays the most critical role in pollen maturation by supplying nutrients to developing microspores. Therefore, a defective tapetum most frequently results in male sterility (Ariizumi and Toriyama 2011).

Both CMS and GMS have been extensively utilized for economical production of F_1 hybrid seeds in many crop species (Bohra et al. 2016; Wan et al. 2019). Typically, a three-line system is used to produce F_1 hybrid seeds via male sterility. A male-sterile line is used as a maternal parent of F_1 hybrids. A near-isogenic and male-fertile maintainer line is required to propagate the male-sterile line in every generation. A male-fertile restorer line is required as a paternal line of F_1 hybrids (Kim and Zhang 2018). Although limited in some crops such as rice, a two-line system in which male fertility of a maternal line is reversible depending on temperature and photoperiod, has been utilized in F_1 hybrid breeding (Kim and Zhang 2018; Zheng et al. 2020). Recently, several biotechnology-based male-sterility systems have also been developed to increase the efficiency of GMS systems (Wu et al. 2016; Zhang et al. 2018; Wan et al. 2019).

In radish (*Raphanus sativus* L.), only CMS has been used in F_1 hybrid breeding since Ogura (1968) discovered male sterility for the first time in radish. The mitochondrial CMS-inducing gene, *orf138*, and its Rf gene were isolated via cybrid analysis (Bonhomme et al. 1991; Grelon et al. 1994) and map-based cloning (Brown et al. 2003; Desloire et al. 2003; Koizuka et al. 2003), respectively. Another type of CMS, designated Dongbu cytoplasmic and genic male sterility (DCGMS), was identified in our previous study (Lee et al. 2008), and a candidate CMS-associated gene, *orf463*, was identified via comparative analysis of complete mitochondrial genome (Park et al. 2013). In addition, two other CMS types have been reported (Nahm et al. 2005; Shi et al. 2010); however, their relationship with other known CMS is unclear.

Meanwhile, little is known about radish GMS compared with the extensively studied CMS. Two GMS phenotypes have been reported in radish (Wang et al. 2012; Duan et al. 2020). Male-sterile phenotypes of these two GMS resulted from complete degeneration of pollen grains (Wang et al. 2012) and abortive stamen (Duan et al. 2020), respectively. In this study, we reported a novel GMS showing inhibition of anther dehiscence, and the causal gene for male sterility was isolated via a map-based cloning approach. The study presents the underlying mechanisms of male-sterility induction and application of novel GMS in radish breeding programs.

Materials And Methods

Plant materials

A new CMS (DCGMS) was identified, and the CMS plants were cross-pollinated with diverse breeding lines in the previous study (Lee et al. 2008). Based on these F_1 populations, a segregating population was generated from the cross [(CMS × R109) × (CMS × R121)]. Both CMS and novel male-sterile phenotypes

were identified in this population. Three of each F_2 and BC_1F_1 population were produced from three heterozygous male-fertile and three male-sterile plants selected from the segregating population reported in the previous study (Lee et al. 2014). A large-sized segregating population was obtained via self-pollination of heterozygous plants in the isolated greenhouse. Genotypes of heterozygous plants were identified using a linked molecular marker (ILP14010). A total of 7,511 plants were analyzed to identify recombinants for fine mapping.

A total of 120 accessions with assigned plant introduction (PI) numbers from Agricultural Research Service (ARS)-Germplasm Resources Information Network (GRIN), USA, were analyzed to identify the accessions containing the recessive allele responsible for the novel male sterility. Accessions with PI numbers are listed in Supplementary Table 1. The total genomic DNA of these accessions was extracted from bulk leaf samples of three randomly selected individual plants in a previous study (Kim et al. 2009).

Evaluation of male-fertility phenotypes and microscopic examination of flower morphology

Seedlings germinated in 128-cell plug trays were transplanted to small pots in the greenhouse. Floral meristem was induced by vernalization during winter. Male fertility of plants was visually observed, and at least five open flowers were evaluated in a single plant. Morphology of anthers was observed with a dissecting microscope (Stemi 2000-C; ZEISS, Oberkochen, Germany). Pollen morphology was analyzed using a scanning electron microscope (SEM, JSM-IT300; JEOL, Tokyo, Japan). Pollen viability was assessed using a lactophenol-aniline blue solution (Kearns and Inouye 1993), and stained pollen grains were observed using an optical microscope (DM LS2; Leica, Wetzlar, Germany).

Analysis of molecular markers and sequencing of PCR products

Total genomic DNAs were extracted from leaf tissues using a cetyl trimethylammonium bromide (CTAB) method (Doyle and Doyle 1987). The analysis of molecular markers was performed via PCR amplification in a 10 µL reaction mixture containing 0.05 µg DNA template, 1.0 µL 10x PCR buffer, 0.2 µL forward primer (10 µM), 0.2 µL reverse primer (10 µM), 0.2 µL dNTPs (10 mM each), and 0.25 U Taq polymerase (Prime Tag DNA polymerase; GeNet Bio, Nonsan, Republic of Korea). Primer sequences of molecular markers are listed in Supplementary Table 2. PCR conditions consisted of an initial denaturation step at 95°C for 4 min; 10 cycles at 95°C for 30 s, 65°C (0.8°C decrements in each cycle) for 30 s and 72°C for 1 min; 35 cycles at 95°C for 30 s, 57°C for 30 s and 72°C for 1 min; and a final 10 min extension step at 72°C. In the case of cleaved amplified polymorphic sequence (CAPS) markers, PCR products were digested with the respective restriction enzymes at 37°C for 1 h. PCR products were visualized on 1.5% agarose gels after ethidium bromide staining or with a Fragment Analyzer™ (Advanced Analytical Technologies, Inc., Ankeny, IA, USA).

Regarding sequencing of PCR products, the PCR components and conditions were similar to those used in the analysis of molecular markers with minor modifications. The volume of reaction mixture was 25 µL, and high-quality Taq polymerase (Advantage 2 Polymerase Mix; Takara Bio, Shiga, Japan) was used.

PCR products were purified using a QIAquick PCR Purification Kit (QIAGEN, Valencia, CA, USA), and the sequencing reactions were conducted by a specialized company (Macrogen, Seoul, Republic of Korea).

RNA extraction and real-time RT-PCR

Total RNAs were extracted from floral buds of male-fertile and male-sterile individuals using an RNeasy Plant Mini Kit (QIAGEN). Bulk samples of diverse developmental stages of floral buds were used for RNA extraction. The cDNAs were synthesized using a cDNA synthesis kit (SuperScript™ III first-strand synthesis system for RT-PCR, Invitrogen, Carlsbad, CA, USA). Real-time RT-PCR was performed using SYBR® Green Realtime PCR Master Mix (Toyobo Co. Ltd, Osaka, Japan) and a LightCycler®96 Real-Time PCR system (Roche Molecular Systems, Pleasanton, CA, USA) according to manufacturers' instructions with four technical replicates. The 100-fold diluted cDNAs were used as templates. A radish gene (Rs395780) encoding a tubulin protein was used as an internal control. The tubulin gene was identified by homology search from the radish draft genome sequences (Jeong et al. 2016). Primer sequences used in real-time RT-PCR are listed in Supplementary Table 3.

Gene transcription levels were also determined via RNA-seq analysis performed in a previous study (Lee et al. 2014). Bulk RNAs of 10 F_2 individuals of each group of male-fertile and male-sterile plants were used in RNA-seq (Lee et al. 2014). The homologous genes were identified from the radish unigene set (Shen et al. 2013), which was used as a reference in RNA-seq, and the RPKM values of corresponding genes were used as units of expression levels.

Construction of a phylogenetic tree

Deduced amino acid sequences of PPR genes isolated from radish and other species were aligned using BioEdit software (Hall 1999). Large gaps in the alignments were removed using Gblocks software (Castresana 2000). A phylogenetic tree was constructed using MEGA version X (Kumar et al. 2018) via neighbor-joining method. Node support of the phylogenetic tree was assessed with 1,000 bootstrap replicates.

Results

Identification of a novel male-sterility phenotype in radish

Two different phenotypes of male sterility were observed in one of the populations containing the DCGMS cytoplasm. In addition to the male-sterile phenotype conferred by the DCGMS cytoplasm reported in the previous study (Lee et al. 2008), another male-sterile phenotype more similar to that of normal flowers was identified (Fig. 1). In contrast to shrunken anthers of DCGMS (Figs. 1C, 1F), anthers of the new male sterility were normal in size, and the surface of anthers was smooth and inflated (Figs. 1B, 1E). However, no pollen grain was observed in dehisced anthers compared with normal male-fertile dehisced anthers showing ample pollen grains (Figs. 1A, 1D).

When the new male-sterile anthers were dissected with a razor blade, an abundance of pollen grains were detected inside anthers. Pollen morphology of the new male sterility analyzed with electron microscopy was indistinguishable from that of male-fertile pollen grains (Figs. 1G, 1H, 1J, 1K). In addition, pollen grains of male-sterile plants were densely stained with an anillin blue solution (Supplementary Fig. 1B), and seeds were normally set when extracted pollen grains were used in artificial self-pollination (Supplementary Fig. 1C), proving viability of pollen grains of male-sterile plants. However, the pollen grains of DCGMS were significantly smaller than those of male-fertile plants (Figs. 1I, 1L). Based on anther and pollen morphologies, the novel male-sterile phenotype was assumed to be attributed to inhibition of anther dehiscence.

Inheritance patterns of novel male sterility and identification of underlying genomic regions and identification of genomic regions containing the RsMs1 locus

The novel male-sterile phenotype was identified, and the male-sterile phenotype in a F_3 population was found to resemble that of the novel male sterility identified in this study. The F_3 population was used to map the Rf gene of DCGMS in a previous study (Lee et al. 2014). Indeed, the morphology of male-sterile plants in this F_3 population was identical to that of the novel male sterility rather than DCGMS. To validate the inheritance of the novel male sterility gene, three heterozygous male-fertile plants were self- and cross-pollinated with male-sterile plants. Segregation ratios were fitted into a single-gene inheritance (Supplementary Table 4). Hereafter, the locus controlling the novel male sterility is designated as *RsMs1* (R*aphanus* s*ativus* M*ale* s*terility 1*).

Based on the genomic region tagged in the previous study (Lee et al. 2014), nine additional markers were developed using information derived from two radish draft genome sequences (Mitsui et al. 2015; Jeong et al. 2016) to delimit the region containing the *RsMs1* locus (Fig. 2A, Supplementary Table 2). Among them, genotypes of the ILP14010 marker were perfectly matched with phenotypes of 179 plants in the self- and cross-pollinated populations, except for four male-fertile plants (MF1F2-16, MS3xMF3-16, MS3xMF3-18, and MS3xMF3-22). Interestingly, the genotypes of nine flanking markers in these four plants were all homozygous recessive, implying that these four plants were probably male-fertile revertants rather than recombinants (Fig. 2B).

A large segregating population was produced by self-pollination of heterozygous male-fertile plants for fine mapping. When phenotypes of 1,911 plants were examined, their segregation ratio was fitted into a single-gene inheritance, and two markers (ILP13570 and ILP14010) showed a perfect linkage to the *RsMs1* locus (Supplementary Table 5). To delimit the region harboring the *RsMs1* locus, recombinants between ILP8045 and ILP14205 were screened (Fig. 2B). Based on these recombinants, the genomic region was delimited between ILP13570 and CAPS14075 markers (Fig. 2). The length of the delimited region was approximately 200–250 kb in the radish draft genome sequences (Fig. 2A). Due to the plethora of genes in the delimited region (Supplementary Fig. 2), 5,600 additional plants in the same segregating population were analyzed using ILP13570 and ILP14205 markers to further narrow down the region, and 48 recombinants were identified. Four additional markers were developed based on draft

genome sequences (Fig. 3A). No recombinants were identified between male-fertility phenotypes and two tightly linked markers (SNP21814 and SNP21812). Therefore, the region containing the *RsMs1* locus was further delimited between IND21816 and CAPS13940 markers (Fig. 3A).

Identification of a candidate gene for the RsMs1 locus in the delimited region and development of a molecular marker for genotyping of the RsMs1 locus

Using draft genome sequences as references, approximately 27-kb delimited regions between IND21816 and CAPS13940 markers were sequenced from individuals containing homozygous dominant and recessive *RsMs1* genotypes, respectively. Nucleotide sequences of dominant and recessive alleles were deposited in the GenBank database under the accession numbers MW036694 and MW036695. A total of 119 single nucleotide polymorphisms (SNPs) and insertions/deletions (InDels) were identified between two allele sequences, but the majority of SNPs and InDels were clustered at the 3' end of the delimited region (Fig. 3B). Based on a 388-bp InDel, an additional marker (IND295320) was developed. Two recombinants were found between this marker and phenotypes, further delimiting the region within a 24-kb range.

Six putative genes were identified in the 24-kb delimited region (Fig. 3B). Among them, one gene (Rs295360) was predicted to encode a PPR protein. In addition, this PPR protein was assumed to be targeted into mitochondria based on the results of three prediction software programs (Supplementary Table 6). However, this gene was unlikely to be the causal gene since there was no polymorphism in the coding and promoter regions between male-fertile and male-sterile alleles (Fig. 3B). In addition, this PPR-coding protein was distantly related to Rf-PPR proteins isolated from other plant species and *Arabidopsis* Rf-like PPRs (Supplementary Fig. 3). Furthermore, this PPR-coding gene was rarely expressed in the floral buds (Fig. 4).

Four genes (RSG21816, Rs295350, Rs295340, and Rs295330) were expressed in floral buds, but only Rs295350 showed significant differential expression between male-fertile and male-sterile F_2 individuals (Fig. 4). An eight-fold increased expression of this gene in the male-fertile bulk RNA was also detected in the RNA-Seq analysis (Supplementary Table 6). A single SNP was detected in the exon3 of Rs295350, but the SNP did not induce any amino acid change. However, a 955-bp insertion was identified in the 7.5 kb upstream region of the male-sterile allele (Fig. 3B). Since there was no significant polymorphism around Rs295350 except for the 955-bp insertion, the reduced transcription was attributed to this insertion. A highly conserved 235-bp motif was identified 249 bp downstream of this insertion via pairwise comparison of syntenic sequences of *Brassica rapa*, *B. oleracea*, and *Arabidopsis* (Fig. 5). Nucleotide sequences of this 235-bp motif were as conserved as the coding sequences of the Rs295350 homologs (Supplementary Table 7).

The 955-bp insertion carried neither the coding sequences nor any features of transposable elements. However, more than 100 copies of this insertion were identified in the draft genome sequence (Fig. 6A). The Rs295350 encodes a transcription factor MYB26-like protein. Since the *Arabidopsis* homolog

(*MYB26*) is positioned at the syntenic region (Supplementary Fig. 4), and is known to play a critical role in anther dehiscence (Yang et al. 2017), the Rs295350 is probably the causal gene associated with the *RsMs1* locus. In addition, the expression levels of radish homologs of the *Arabidopsis* downstream genes underlying the secondary thickening and dehiscence of anthers were generally reduced (Supplementary Fig. 5, Supplementary Table 8). Likewise, reduced transcription of these genes was observed in *Arabidopsis MYB26* mutants (Yang et al. 2017). Hereafter, the Rs295360 is designated *RsMYB26*.

A combination of three primers was designed based on the 955-bp insertion to develop a simple PCR marker for genotyping of the *RsMs1* locus (Fig. 6A). Since the intensities of recessive allele-linked PCR products were significantly lighter than those of dominant allele-linked products in heterozygotes possibly due to the presence of multiple copies of this insertion, a single mismatched nucleotide was inserted in the RsMs-F1 primer. As a result, the intensities of PCR products of both alleles were parallel (Fig. 6B). This marker was designated RsMs1, which was used to genotype the original population from which the novel male sterility was first identified. All homozygous recessive genotypes showed the novel male-sterile phenotype; however, the DCGMS phenotype was observed in the three heterozygous individuals (Table 1), suggesting that the two types of male sterility were controlled by independent loci. In addition, the RsMs1 marker was used to survey the distribution of the recessive *RsMs1* allele among 120 diverse PI accessions (Supplementary Table 1). The recessive alleles were detected in 11 accessions in a heterozygous state, and five of them originated in Afghanistan (Supplementary Table 1).

Discussion

Identification of the gene responsible for novel male sterility in radish via map-based cloning

A novel male-sterile phenotype was identified in one of populations containing the DCGMS cytoplasm, and large segregating populations were used to delimit the region containing the causal gene in this study. Two radish draft genome sequences were utilized to identify the candidate genes. In the delimited regions, most genes were collinear between two radish draft genome sequences, although the position of a few genes was not consistent between them. Collinearity was also conserved between radish and *Arabidopsis* genomes (Supplementary Fig. 2), implying reliable assembly of the *RsMs1*-flanking regions in the two radish draft genome sequences (Mitsui et al. 2015; Jeong et al. 2016). These draft genome sequences enabled successful identification of the causal gene without expensive and tedious genomic DNA library construction such as bacterial artificial chromosome (BAC).

A gene coding for a MYB transcription factor, orthologous to the *Arabidopsis MYB26* gene, was identified as the causal gene for the novel male sterility identified in this study. Since radish is not amenable to *Agrobacterium*-mediated transformation, the verification of candidate gene function via a complementation test using genetic transformation is intractable in radish. However, several lines of evidences establishing the role of *RsMYB26* gene in male sterility induction were presented in this study. First, the phenotype of the novel male sterility was almost identical to that of *Arabidopsis* male-sterile

mutants harboring inactive *MYB26* genes. Since the first *MYB26* mutant was induced by mutagenesis in *Arabidopsis* (Dawson et al. 1993), the *MYB26* has been verified as the gene associated with male sterility via DNA transposon tagging in *Arabidopsis* (Steiner-Lange et al. 2003). Subsequently, the role of *MYB26* in male gametophyte development was extensively studied (Yang et al. 2007, 2017).

Unlike most male-sterile mutants in which pollen grains were non-viable, the male sterility of the *MYB26* mutants was caused by inhibition of anther dehiscence. Pollen morphology of the mutants was indistinguishable from that of normal pollen, and pollen grains were fully functional (Steiner-Lange et al. 2003). Likewise, no anther dehiscence occurred, and pollen morphologies were normal in the novel male sterility identified in this study. Viability of pollen grains of male-sterile plants were confirmed by aniline blue staining and artificial self-pollination of male-sterile plants (Supplementary Fig. 1). The *RsMs1* genotypes of progenies produced from artificial pollination were all homozygous recessive (Supplementary Fig. 1C), indicating that parents of these progenies were all male-sterile plants.

The anther wall consists of four cell layers: epidermis, endothecium, middle layer, and tapetum. The *Arabidopsis MYB26* gene regulates the genes involved in secondary thickening of the endothecium (Yang et al. 2007, 2017). A reduced expression of these downstream genes was observed in the *MYB26* mutants. Similarly, the transcription of radish gene homologs was generally reduced in the male-sterile radish (Supplementary Fig. 5, Supplementary Table 8). During anther dehiscence, epidermal dehydration and endothecium thickening generate forces in the anther wall, resulting in anther opening and pollen release (Nelson et al. 2012). Therefore, the *MYB26* gene is essential for successful anther dehiscence.

A significantly reduced transcription of the *RsMYB26* was observed in the novel male-sterile radish (Fig. 4). The conserved synteny of genomic regions flanking the *MYB26* gene between radish and *Arabidopsis* indicates that the *RsMYB26* is probably orthologous to the *Arabidopsis MYB26* (Supplementary Fig. 4). Interestingly, we found no critical mutations in the coding and putative promoter sequences of the *RsMYB26* gene except for a 955-bp insertion located 7.5 kb upstream. A couple of scenarios may explain the reduced expression.

First, a putative transcriptional enhancer is situated around the 7.5 kb upstream region, and binding of other transcription factors to this enhancer is blocked by the 955-bp insertion. Indeed, a highly conserved motif was identified 249 bp downstream of this insertion (Fig. 5). Further studies are required to confirm the role of this motif. Indirectly, the effects of this motif on the expression of *MYB26* gene can be evaluated using *Arabidopsis*. Compared with enhancer sequences in animals, little is known about plant enhancers. Dozens of plant enhancers have been characterized until now (Weber et al. 2016). Similar to the highly conserved motif identified in this study, the P1-rr distal enhancer in maize is located in the 6 kb upstream region of the target gene (Sidorenko et al. 1999). The upstream intergenic regions of *MYB26* orthologs were relatively lengthy compared with those of other flanking genes in both radish and *Arabidopsis* (Supplementary Fig. 4). The corresponding regions in *B. rapa* and *B. oleracea* were extended further (Fig. 5). Therefore, these intergenic regions might be valuable in studies analyzing the role of plant enhancers in the future.

Alternatively, the insertion of the 955-bp repeat may induce DNA methylation of the flanking regions including enhancers and possibly promoter. DNA methylation is known to regulate silencing of transposable elements, repetitive sequences, and transgenes in plants (Bartels et al. 2018). Although we failed to identify any features of transposable elements in the 955-bp insertion, this repeat may play a role in triggering DNA methylation since more than 100 copies of this insertion were identified in the radish genome (Fig. 6A). Otherwise, the microRNAs regulating the expression of *RsMYB26* might be inactivated by the 955-bp insertion. MicroRNAs are known to play an important role in the regulation of gene expression in plants (Wang et al. 2019). Further studies are required to elucidate the cause of reduced *RsMYB26* gene transcription.

Application of novel male sterility in radish breeding programs

Morphological features and the causal gene of novel male sterility identified in this study indicate that this male sterility is GMS rather than CMS. The advantages of GMS outweigh those of CMS. Introgression of GMS into other elite lines is relatively easy since the cytoplasm types are not considered necessary. In addition, more diverse combinations of parental lines of F_1 hybrids can be designed, since most breeding lines can be used as restorer lines. Further, GMS can be used to develop an efficient two-line system in which a maintainer line is unnecessary since male fertility of GMS in maternal lines can be restored by environmental factors such as temperature and photoperiod (Kim and Zhang 2018). We observed that the male sterility of four plants reverted to male fertility due to unknown reasons (Fig. 2). This GMS can be utilized to develop a two-line system for F_1 hybrid seed production in radish for the first time if the effects of temperature or photoperiod on the reversion of male sterility are identified in the future.

A reliable molecular marker for genotyping of the *RsMs1* locus was developed in this study. Since this marker was designed based on the 955-bp insertion, it can be classified as a functional marker (Andersen and Lübberstedt 2003). Since there is no recombination between a functional marker and the target traits, functional markers are useful in predicting the correct genotypes of plants even without known pedigree (Salgotra and Stewart 2020). Indeed, we found 11 accessions carrying the recessive *RsMs1* alleles using this marker. Taken together, the novel GMS and its functional marker developed in this study represent valuable resources for radish breeding programs.

Declarations

Acknowledgments

The authors thank Ji-hwa Heo, Jeong-An Yoo, and Su-jeong Kim for their dedicated technical assistance.

Authors' contribution

Seongjun Kim performed experiments and drafted the manuscript. Sunggil Kim organized and coordinated this research project and edited the final manuscript.

Funding

This study was supported by the Korea Institute of Planning and Evaluation for Technology in Food, Agriculture and Forestry (IPET) via Golden Seed Project (Center for Horticultural Seed Development, No 213007-05-5-SBB10) along with a grant from the Next-Generation BioGreen 21 Program (Plant Molecular Breeding Center No. PJ013400).

Data availability

Not applicable

Ethics approval

All experiments were performed in compliance with current laws of the Republic of Korea.

Consent for publication

Not applicable.

Competing interests

The authors declare no competing interest.

References

1. Andersen JR, Lübberstedt T (2003) Functional markers in plants. Trends Plant Sci 8:554-560
2. Ariizumi T, Toriyama K (2011) Genetic regulation of sporopollenin synthesis and pollen exine development. Annu Rev Plant Biol 62:437-460
3. Bartels A, Han Q, Nair P, Stacey L, Gaynier H, Mosley M, Huang QQ, Pearson JK, Hsieh T, An YC, Xiao W (2018) Dynamic DNA methylation in plant growth and development. Int J Mol Sci 19:2144
4. Bentolila S, Alfonso AA, Hanson MR (2002) A pentatricopeptide repeat-containing gene restores fertility to cytoplasmic male-sterile plants. Proc Natl Acad Sci USA 99:10887-10892
5. Bohra A, Jha UC, Adhimoolam P, Bisht D, Singh NP (2016) Cytoplasmic male sterility (CMS) in hybrid breeding in field crops. Plant Cell Rep 35:967-993
6. Bonhomme S, Budar F, Ferault M, Pelletier G (1991) A 2.5 kb *Nco* I fragment of Ogura radish mitochondrial DNA is correlated with cytoplasmic male-sterility in *Brassica* cybrids. Curr Genet 19:121-127
7. Brown GG, Formanova N, Jin H, Wargachuk R, Dendy C, Patil P, Laforest M, Zhang J, Cheung WY, Landry BS (2003) The radish *Rfo* restorer gene of Ogura cytoplasmic male sterility encodes a protein with multiple pentatricopeptide repeats. Plant J 35:262-272
8. Budar F, Touzet P, de Paepe R (2003) The nucleo-mitochondrial conflict in cytoplasmic male sterilities revised. Genetica 117:3-16

9. Castresana J (2000) Selection of conserved blocks from multiple alignments for their use in phylogenetic analysis. Mol Biol Evol 17:540-552
10. Cho Y, Lee Y, Park B, Han T, Kim S (2012) Construction of a high-resolution linkage map of *Rfd1*, a restorer-of-fertility locus for cytoplasmic male sterility conferred by DCGMS cytoplasm in radish (*Raphanus sativus* L.) using synteny between radish and *Arabidopsis* genomes. Theor Appl Genet 125:467-477
11. Dawson J, Wilson ZA, Aarts MGM, Braithwaite AF, Briarty LG, Mulligan BJ (1993) Microspore and pollen development in six male-sterile mutants of *Arabidopsis thaliana*. Can J Bot 71:629-638
12. Desloire S, Gherbi H, Laloui W, Marhadour S, Clouet V, Cattolico L, Falentin C, Giancola S, Renard M, Budar F, Small I, Caboche M, Delourme R, Bendahmane A (2003) Identification of the fertility restoration locus, *Rfo*, in radish, as a member of the pentatricopeptide-repeat protein family. EMBO Rep 4:588-594
13. Doyle JJ, Doyle JL (1987) A rapid DNA isolation procedure for small quantities of fresh leaf tissue. Phytochem Bull 19:11-15
14. Duan N, Bai J, Xie K, Wang J, Wang X (2020) *De novo* and comparative transcriptome analysis of genetic male sterile and fertile lines in radish (*Raphanus sativus*). J Hort Sci Biotechnol 95:32-43
15. Fujii S, Bond CS, Small ID (2011) Selection patterns on restorer-like genes reveal a conflict between nuclear and mitochondrial genomes throughout angiosperm evolution. Proc Natl Acad Sci USA 108:1723-1728
16. Gaborieau L, Brown GG, Mireau H (2016) The propensity of pentatricopeptide repeat genes to evolve into restorers of cytoplasmic male sterility. Front Plant Sci 7:1816
17. Grelon M, Budar F, Bonhomme S, Pelletier G (1994) Ogura cytoplasmic male-sterility (CMS)-associated *orf138* is translated into a mitochondrial membrane polypeptide in male-sterile *Brassica* cybrids. Mol Gen Genet 243:540-547
18. Hall TA (1999) BioEdit: a user-friendly biological sequence alignment editor and analysis program for Window 95/98/NT. Nucl Acids Symp Ser 41:95-98
19. Hanson MR, Bentolila S (2004) Interactions of mitochondrial and nuclear genes that affect male gametophyte development. Plant Cell 16:154-169
20. Jeong Y, Kim N, Ahn BO, Oh M, Chung W, Chung H, Jeong S, Lim K, Hwang Y, Kim G, Baek S, Choi S, Hyung D, Lee S, Sohn S, Kwon S, Jin M, Seol Y, Chae WB, Choi KJ, Park B, Yu H, Mun J (2016) Elucidating the triplicated ancestral genome structure of radish based on chromosome-level comparison with the *Brassica* genomes. Theor Appl Genet 129:1357-1372
21. Kearns CA, Inouye DW (1993) Techniques for pollination biologists. University Press of Colorado. pp. 111-111
22. Kim S, Lee Y, Lim H, Ahn Y, Sung S (2009) Identification of highly variable chloroplast sequences and development of cpDNA-based molecular markers that distinguish four cytoplasm types in radish (*Raphanus sativus* L.). Theor Appl Genet 119:189-198

23. Kim Y, Zhang D (2018) Molecular control of male fertility for crop hybrid breeding. Trends Plant Sci 23:53-65
24. Klein RR, Klein PE, Mullet JE, Minx P, Rooney WL, Schertz KF (2005) Fertility restorer locus *Rf1* of sorghum (*Sorghum bicolor* L.) encodes a pentatricopeptide repeat protein not present in the collinear region of rice chromosome 12. Theor Appl Genet 111:994-1012
25. Koizuka N, Imai R, Fujimoto H, Hayakawa T, Kimura Y, Kohno-Murase J, Sakai T, Kawasaki S, Imamura J (2003) Genetic characterization of a pentatricopeptide repeat protein gene, *orf687*, that restores fertility in the cytoplasmic male-sterile Kosena radish. Plant J 34:407-415
26. Komori T, Ohta S, Murai N, Takakura Y, Kuraya Y, Suzuki S, Hiei Y, Imaseki H, Nitta N (2004) Map-based cloning of a fertility restorer gene, *Rf-1*, in rice (*Oryza sativa* L.). Plant J 37:315-325
27. Kumar S, Stecher G, Li M, Knyaz C, Tamura K (2018) MEGA X: Molecular evolutionary genetics analysis across computing platforms. Mol Biol Evol 35:1547-1549
28. Laser KD, Lersten NR (1972) Anatomy and cytology of microsporogenesis in cytoplasmic male sterile angiosperms. Bot Rev 38:425-454
29. Lee Y, Cho Y, Kim S (2014) A high-resolution linkage map of the *Rfd1*, a restorer-of-fertility locus for cytoplasmic male sterility in radish (*Raphanus sativus* L.) produced by a combination of bulked segregant analysis and RNA-Seq. Theor Appl Genet 127:2243-2252
30. Lee Y, Park S, Lim C, Kim H, Lim H, Ahn Y, Sung S, Yoon M, Kim S (2008) Discovery of a novel cytoplasmic male-sterility and its restorer lines in radish (*Raphanus sativus* L.). Theor Appl Genet 117:905-913
31. Mitsui Y, Shimomura M, Komatsu K, Namiki N, Shibata-Hatta M, Imai M, Katayose Y, Mukai Y, Kanamori H, Kurita K, Kagami T, Wakatsuki A, Ohyanagi H, Ikawa H, Minaka N, Nakagawa K, Shiwa Y, Sasaki T (2015) The radish genome and comprehensive gene expression profile of tuberous root formation and development. Sci Rep 5:10835
32. Nahm S, Lee H, Lee S, Joo G, Harn C, Yang S, Min B (2005) Development of a molecular marker specific to a novel CMS line in radish (*Raphanus sativus* L.). Theor Appl Genet 111:1191-1200
33. Nelson MR, Band LR, Dyson RJ, Lessinnes T, Wells DM, Yang C, Everitt NM, Jensen OE, Wilson ZA (2012) A biomechanical model of anther opening reveals the roles of dehydration and secondary thickening. New Phytol 196:1030-1037
34. Ogura H (1968) Studies on the new male sterility in Japanese radish, with special reference to the utilization of this sterility towards the practical raising of hybrid seeds. Mem Fac Agr Kagoshima Univ 6:39-78
35. Park JY, Lee Y, Lee J, Choi B, Kim S, Yang T (2013) Complete mitochondrial genome sequence and identification of a candidate gene responsible for cytoplasmic male sterility in radish (*Raphanus sativus* L.) containing DCGMS cytoplasm. Theor Appl Genet 126:1763-1774
36. Salgotra RK, Stewart CN (2020) Functional markers for precision plant breeding. Int J Mol Sci 21:4792

37. Sanders PM, Bui AQ, Weterings K, McIntire KN, Hsu Y, Lee PY, Truong MT, Beals TP, Goldberg RB (1999) Anther developmental defects in *Arabidopsis thaliana* male-sterile mutants. Sex Plant Reprod 11:297-322
38. Schnable PS, Wise RP (1998) The molecular basis of cytoplasmic male sterility and fertility restoration. Trends Plant Sci 3:175-180
39. Shen D, Sun H, Huang M, Zheng Y, Li X, Fei Z (2013) RadishBase: A Database for Genomics and Genetics of Radish. Plant Cell Physiol 54:e3
40. Shi S, Ding D, Mei S, Wang J (2010) A comparative light and electron microscopic analysis of microspore and tapetum development in fertile and cytoplasmic male sterile radish. Protoplasma 241:37-49
41. Sidorenko L, Li X, Tagliani L, Bowen B, Peterson T (1999) Characterization of the regulatory elements of the maize *P-rr* gene by transient expression assays. Plant Mol Biol 39:11-19
42. Steiner-Lange S, Unte US, Eckstein L, Yang C, Wilson ZA, Schmelzer E, Dekker K, Saedler H (2003) Disruption of *Arabidopsis thaliana MYB26* results in male sterility due to non-dehiscent anthers. Plant J 34:519-528
43. Sweigart A (2019) Lactophenol-aniline blue solution. protocols.io. https://dx.doi.org/10.17504/protocols.io.baf4ibqw
44. Wan X, Wu S, Li Z, Dong Z, An X, Ma B, Tian Y, Li J (2019) Maize genic male-sterility genes and their applications in hybrid breeding: progress and perspectives. Mol Plant 12:321-342
45. Wang J, Mei J, Ren G (2019) Plant microRNAs: Biogenesis, Homeostasis, and Degradation. Front Plant Sci 10:360
46. Wang Z, Gao L, Liu HZ, Mei SY, Zhou Y, Xiang CP, Wang T (2012) Genetic and cytological analysis of a new spontaneous male sterility in radish (*Raphanus sativus* L.). Euphytica 186:313-320
47. Weber B, Zicola J, Oka R, Stam M (2016) Plant enhancers: A call for discovery. Trends Plant Sci 21:974-987
48. Wu Y, Fox TW, Trimnell MR, Wang L, Xu R, Cigan AM, Huffman GA, Garnaat CW, Heshey H, Albertsen MC (2016) Development of a novel recessive genetic male sterility system for hybrid seed production in maize and other cross-pollinating crops. Plant Biotechnol J 14:1046-1054
49. Yang C, Song J, Ferguson AC, Klisch D, Simpson K, Mo R, Taylor B, Mitsuda N, Wilson ZA (2017) Transcription factor MYB26 is key to spatial specificity in anther secondary thickening formation. Plant Physiol 175:333-350
50. Yang C, Xu Z, Song J, Conner K, Barrena GV, Wilson ZA (2007) *Arabidopsis MYB26/MALE STERILE35* regulates secondary thickening in the endothecium and is essential for anther dehiscence. Plant Cell 19:534-548
51. Zhang D, Luo X, Zhu L (2011) Cytological analysis and genetic control of rice anther development. J Genet Genomics 38:379-390

52. Zhang D, Wu S, An X, Xie K, Dong Z, Zhou Y, Xu L, Fang W, Liu S, Liu S, Zhu T, Li J, Rao L, Zhao J, Wan X (2018) Construction of a multicontrol sterility system for a maize male-sterile line and hybrid seed production based on the *ZmMs7* gene encoding a PHD-finger transcription factor. Plant Biotechnol J 16:459-471
53. Zheng W, Ma Z, Zhao M, Xiao M, Zhao J, Wang C, Gao H, Bai Y, Wang H, Sui G (2020) Research and development strategies for hybrid *japonica* rice. Rice 13:36

Tables

Table 1. Relationship between RsMs1 marker genotypes and phenotypes of male fertility in the population with novel male sterility first identified.

Genotype of RsMs1 marker[a]	Phenotype of male fertility			Total
	Male-fertile	Male-sterile		
		Novel male sterility	DCGMS	
A	11	0	0	11
H	20	0	3	23
B	0	7	0	7

[a]A: homozygous dominant, H: heterozygous, B: homozygous recessive

Figures

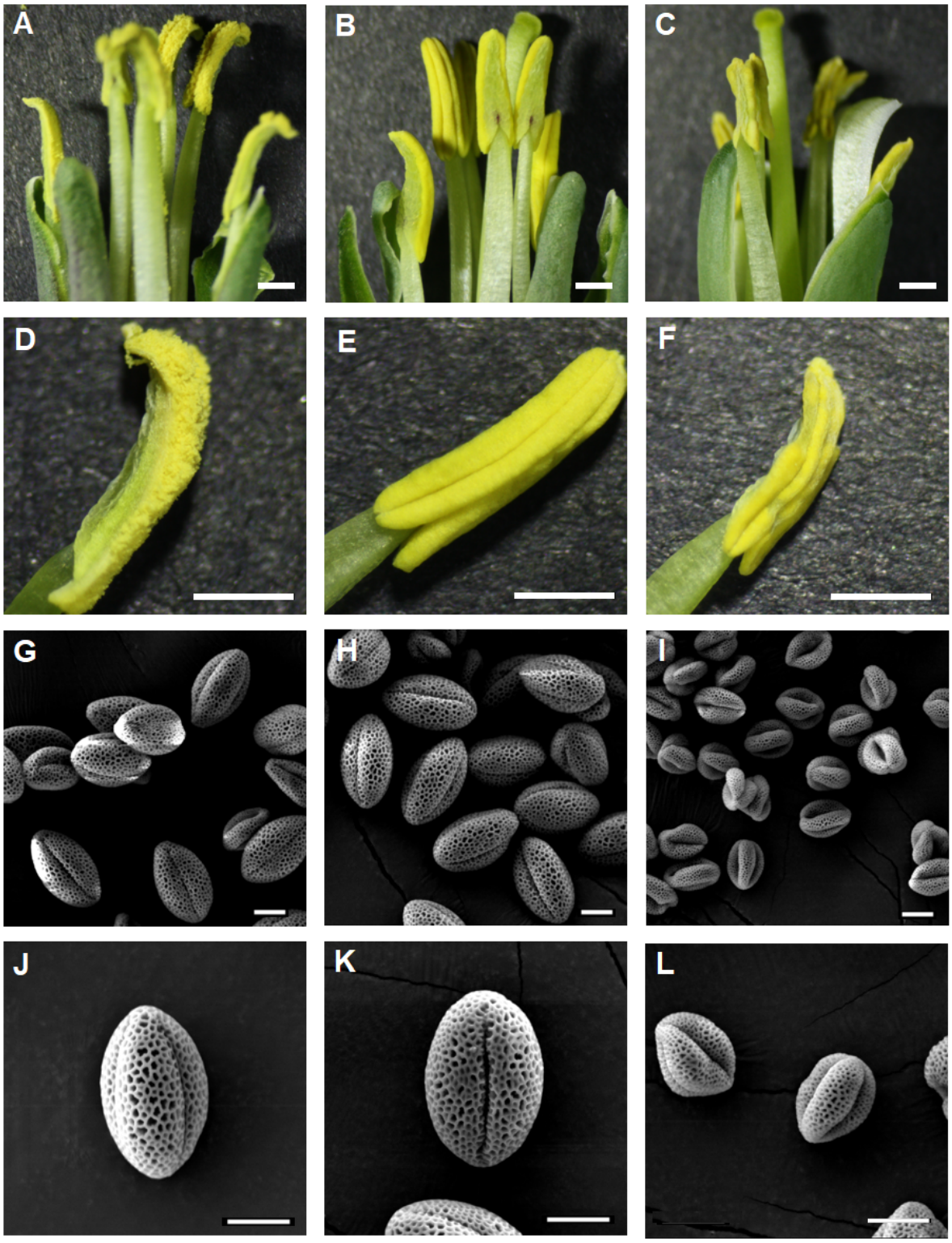

Figure 1

Flower morphology of male-fertile and male-sterile radishes. Male-fertile plants (A, D, G, J), novel male-sterile plants identified in this study (B, E, H, K), plants showing the CMS phenotype conferred by the DCGMS cytoplasm (C, F, I, L). A, B, C: Open flowers in which petals were detached for better visibility. Bars indicate 1 mm. D, E, F: Dehisced anthers. Bars indicate 1 mm. G, H, I: Electron microscopic images of pollen grains. Bars indicate 10 µm. J, K, L: Close-up images of pollen grains. Bars indicate 10 µm.

A

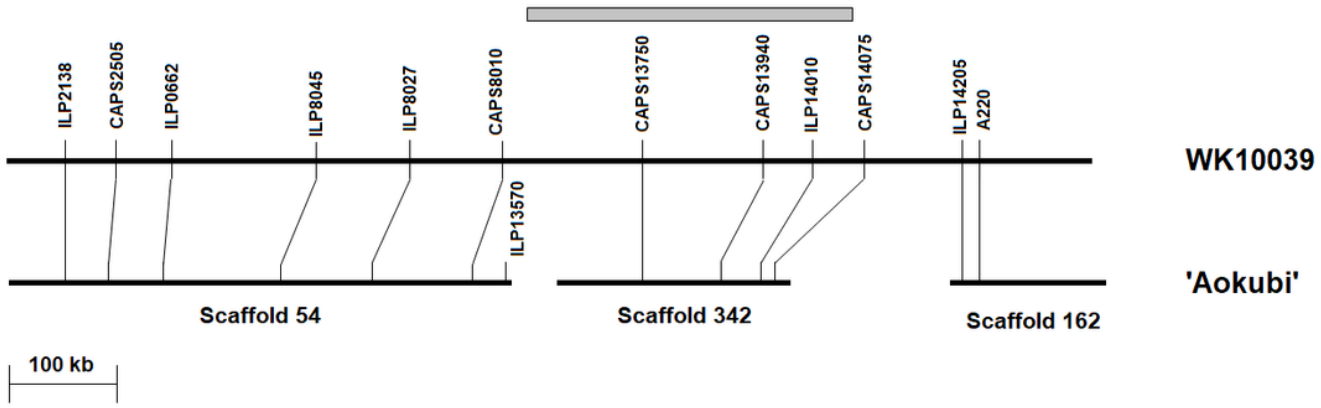

B

Plant	Marker									
	ILP8045	ILP8027	CAPS8010	ILP13570	CAPS13750	CAPS13940	*RsMs1*	ILP14010	CAPS14075	ILP14205
MF1F2-16	B	B	B	B	B	B	D	B	B	B
MS3XMF3-16	B	B	B	B	B	B	D	B	B	B
MS3XMF3-18	B	B	B	B	B	B	D	B	B	B
MS3XMF3-22	B	B	B	B	B	B	D	B	B	B
MF4F2-717	H	B	B	B	B	B	B	B	B	B
MF4F2-950	H	B	B	B	B	B	B	B	B	B
MF4F2-1450	B	H	H	H	H	H	D	H	H	H
MF4F2-1454	H	B	B	B	B	B	B	B	B	B
MF4F2-1411	B	B	H	H	H	H	D	H	H	H
MF4F2-1964	H	H	B	B	B	B	B	B	B	B
MF4F2-189	H	H	B	B	B	B	B	B	B	B
MF2F2-7	B	B	B	B	H	H	D	H	H	H
MF2F2-28	H	H	H	H	B	B	B	B	B	B
MF4F2-1620	B	B	B	B	B	B	B	B	H	H
MF4F2-5	H	H	H	H	H	H	D	H	B	B
MF4F2-961	H	H	H	H	H	H	D	H	H	B
MF4F2-1290	B	B	B	B	B	B	B	B	B	H
MF4F2-176	B	B	B	B	B	B	B	B	B	H

Figure 2

Delimitation of genomic regions harboring the RsMs1 locus. A. Physical maps of the RsMs1-flanking regions of two radish draft genome sequences. A gray rectangular bar indicates the delimited regions via recombinant analysis. ‘WK10039’ and ‘Aokubi’ are radish accessions used to construct draft genome sequences by Jeong et al. (2016) and Mitsui et al. (2015), respectively. ILP2138, CAPS2505, ILP0662, and A220 markers were developed in the previous study (Cho et al. 2012). B. Genotypes of molecular markers and phenotypes of the RsMs1 locus in male-fertile revertants and recombinants selected from segregating populations. Phenotypes of revertants and groups of same genotypes located to the left of the crossover points are shown in gray boxes. A: homozygous dominant, H: heterozygous, B: homozygous recessive, D: homozygous dominant and heterozygous.

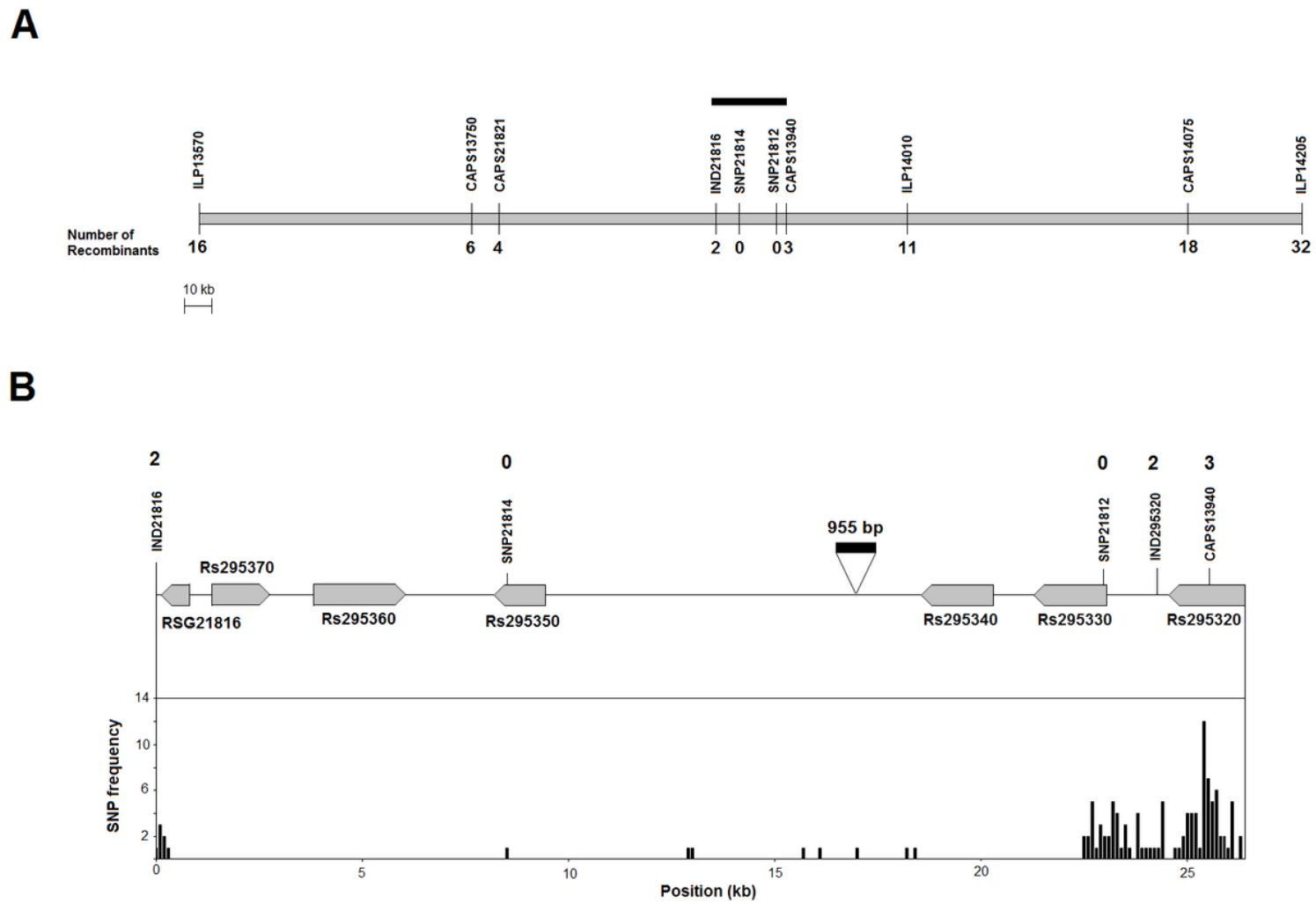

Figure 3

Identification of candidate genes in the delimited regions containing the RsMs1 locus. A. Physical map of the delimited regions. A rectangular black bar indicates the further delimited region shown in Fig. 3B. Numbers under the marker names indicate the number of recombinants between the RsMs1 locus and corresponding markers. B. Genomic organization of finally delimited regions. Arrow-shaped boxes indicate putative genes and 5'-to-3' orientation. Gene IDs beginning with 'RSG' and 'Rs' were designated by Mitsui et al. (2015) and Jeong et al. (2016), respectively, for the genes identified in draft genome sequences. Numbers above the markers indicate the number of recombinants between the RsMs1 locus and corresponding markers. An inverted triangle indicates the position of a 955-bp insertion. Distribution of SNPs or InDels between dominant and recessive RsMs1 alleles is shown under the genomic organization.

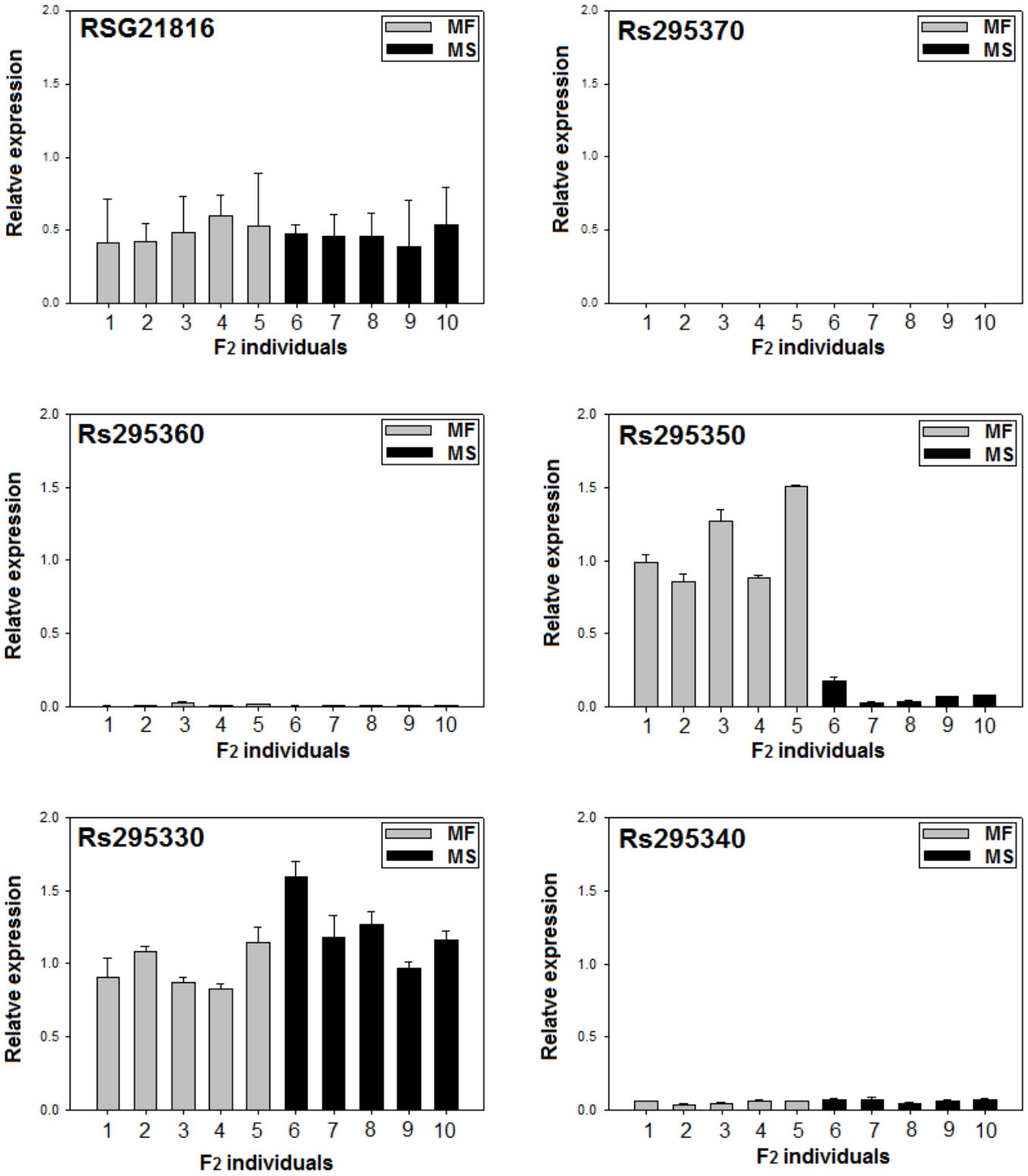

Figure 4

Relative expression of putative genes located in the delimited regions. A gene coding for a tubulin protein was used as an internal control.

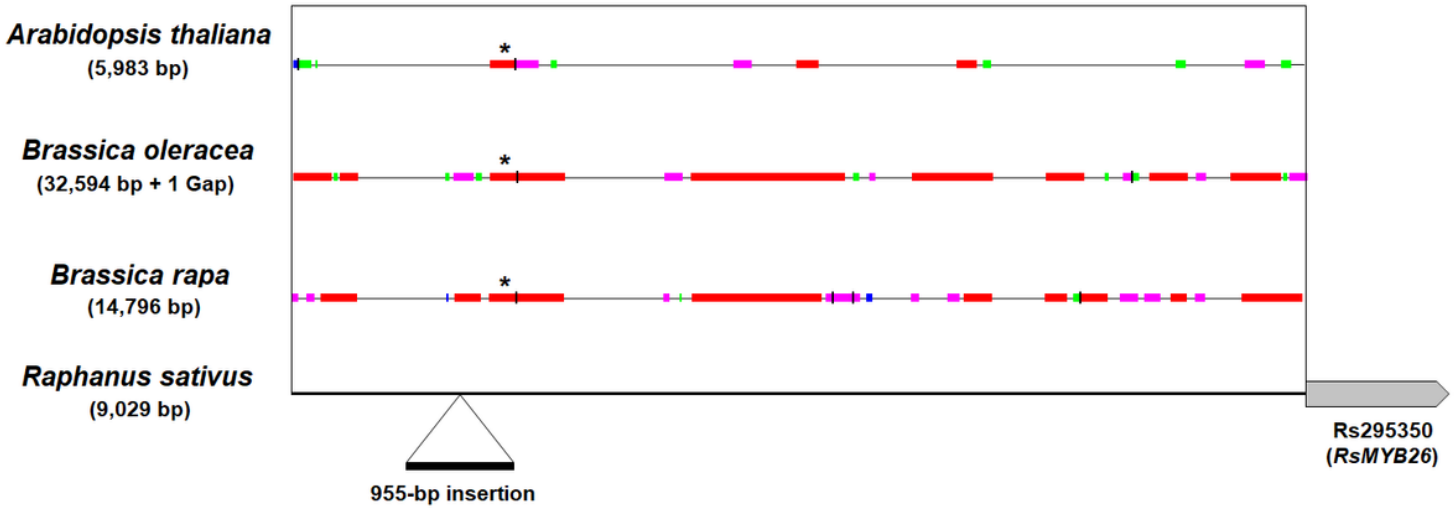

Figure 5

Identification of conserved motifs among radish, Brassica rapa, B. olelacea, and Aradidopsis in the upstream intergenic regions of the RsMYB26 gene. An arrow-shaped box indicates the RsMYB26 gene and 5'-to-3' orientation. A triangle indicates the position of a 955-bp insertion. Lengths of corresponding intergenic regions in each species are shown in parenthesis. Asterisks indicate the locations of a conserved 235-bp motif. Colored boxes above the radish intergenic regions provide graphic summary of NCBI blastn suite-2sequences. Red, pink, green, and blue colors indicate alignment scores ≥ 200, 80-200, 50-80, and 40-50, respectively.

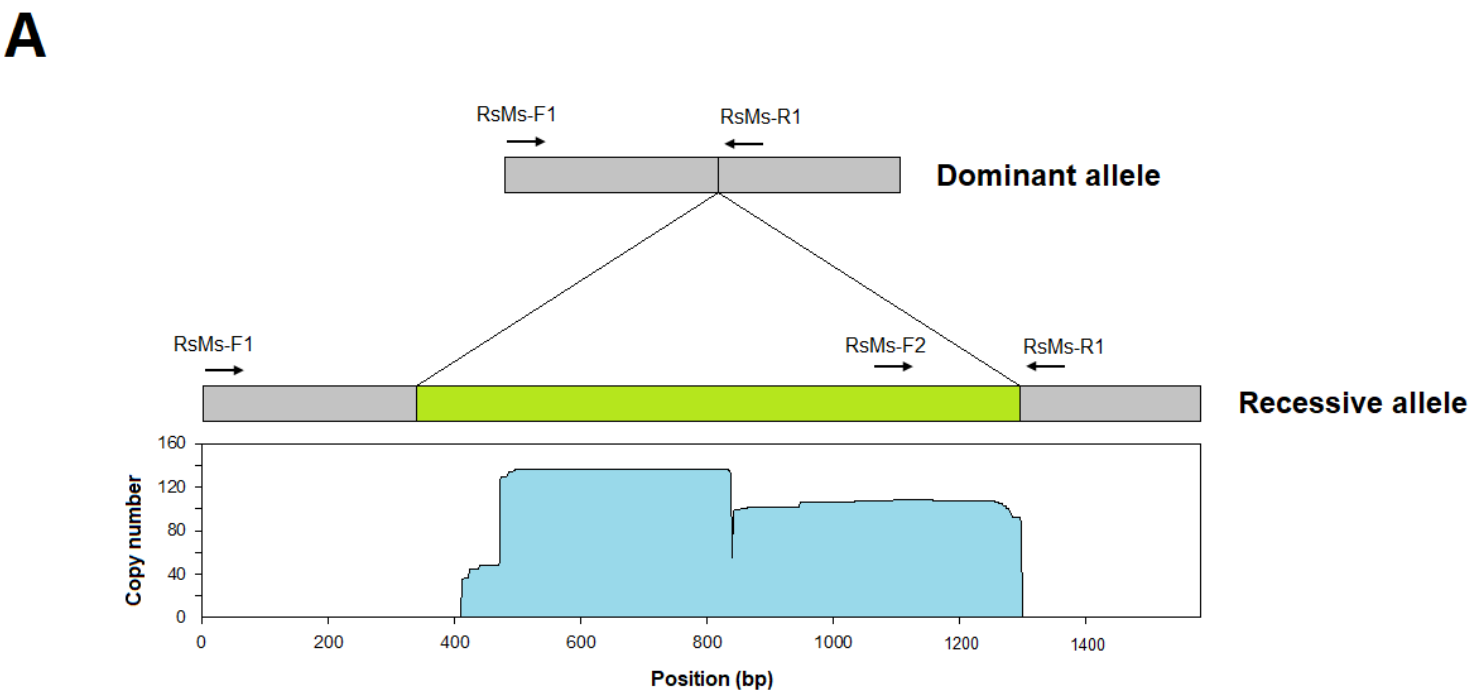

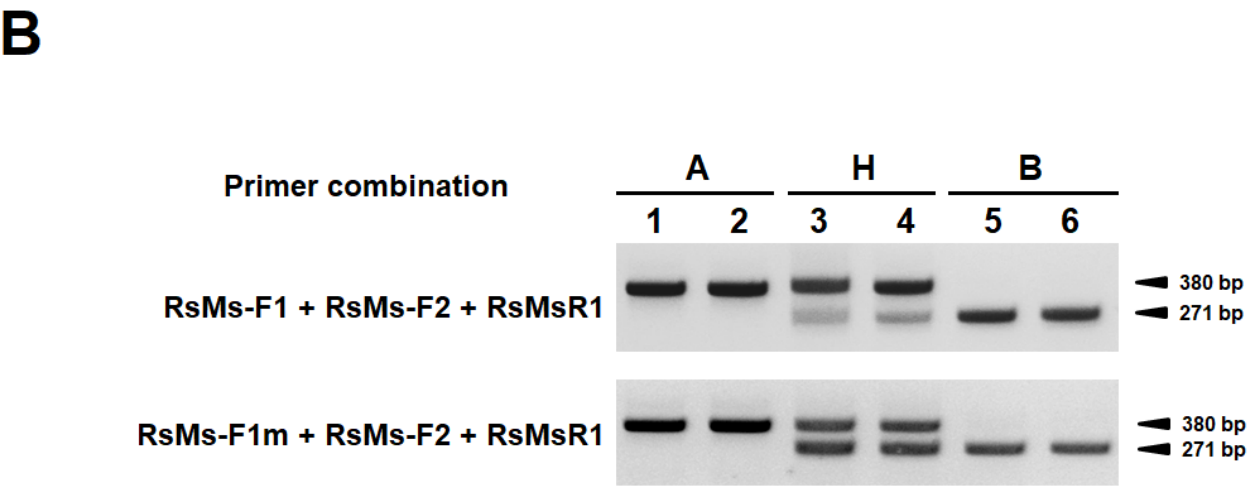

Figure 6

Development of a molecular marker for genotyping the RsMs1 locus. A. Primer positions of the molecular marker and copy number estimation of the 955-bp insertion. Gray and green boxes indicate flanking regions and 955-bp insertion, respectively. Arrows indicate primer-binding sites. Copy numbers of repeat sequences showing homology (E value < 1.0E-100) with the 955-bp insertion are depicted under the recessive allele organization. Repeat sequences were identified from the radish draft genome sequence produced by Jeong et al. (2016). B. PCR products of two primer combinations. The RsMs-F1m is a modified primer containing a single mismatched nucleotide. Primer sequences are listed in Supplementary Table 2. A: homozygous dominant, H: heterozygous, B: homozygous recessive individuals.

Supplementary Files

This is a list of supplementary files associated with this preprint. Click to download.

- SupplementaryFig.1.Pollenviability.tif
- SupplementaryFig.2.synteny.tif
- SupplementaryFig.3.phylogenetictreeofPPRs.tif
- SupplementaryFig.4.Syntenyofdelimitedregions.tif
- SupplementaryFig.5.MYB26relatedgeneexpression.tif
- SupplementaryTable1.ListofPlaccessions.xlsx
- SupplementaryTable2.Listofmolecularmarkers.xlsx
- SupplementaryTable3.PrimersforrealtimePCR.xlsx
- SupplementaryTable4.InheritanceofthenovelMS.docx
- SupplementaryTable5.Inheritanceinalargepopulation.docx
- SupplementaryTable6.genesinthedelimitedregion.xlsx
- SupplementaryTable7.PairwisehomologyofMYB26.docx
- SupplementaryTable8.MYB26relatedgenes.xlsx